Program Digest, 2019 IEEE International Ultrasonics Symposium (IUS)
Glasgow, Scotland, October 6-9, 2019

Polarization conversion of surface acoustic waves for enhanced microscale actuation applications

Robert Weser
Leibniz Institute for Solid State and Materials Research Dresden
SAWLab Saxony
Dresden, Germany
r.weser@ifw-dresden.de

Alexandre Darinskii
Institute of Crystallography FSRC
"Crystallography and Photonics"
Russian Academy of Science
Moscow, Russia
alexandre_dar@mail.ru

Hagen Schmidt
Leibniz Institute for Solid State and Materials Research Dresden
SAWLab Saxony
Dresden, Germany
h.schmidt@ifw-dresden.de

***Abstract*— Surface acoustic wave (SAW) based actuators used for active microfluidic applications, most often utilize Rayleigh-type SAW with significant out-of-plane surface displacements. Besides the desired momentum transfer to the liquid in contact with the active surface, an additional, unwanted momentum transfer into the polymer wall of the microfluidic vessel also occurs. The energy dissipation inside the vessel wall decreases actuator efficiency and may result in leakage and degradation of the wall material. Our first investigations show that boundary polarized SAW modes with comparatively small out-of-plane displacement can also be used for microfluidic actuation purposes to overcome this drawback. The boundary polarized mode is capable to pass the vessel wall-substrate interface with minimum of acoustical loss, but needs to be converted finally inside the vessel into a vertical polarized mode in order to ensure the intended acoustofluidic interaction. Such a mode or polarization conversion can be realized by an appropriate scattering structure arranged inside the vessel area.**

Keywords—surface acoustic wave (SAW), SAW actuator, boundary polarized SAW, vertical polarized SAW, polarization conversion, SAW scattering, Laser Doppler vibrometry

I. INTRODUCTION

Rayleigh-type surface acoustic waves (SAW) are typically used for microscale actuators (e.g. for SAW-driven microfluidics) due to the predominantly vertical polarization (VP), i.e. the mechanical displacement component perpendicular to the surface the SAW propagates along [1]. The corresponding out-of-plane displacement component gives rise to the desired momentum transfer to the liquid in contact with the active surface, but also to the vessel wall usually made of a polymer. The latter fact can result in degradation or delamination of the vessel wall material leading to leakage or even to total destruction of the microfluidic setup, especially at higher SAW power.

One promising approach to overcome this drawback is to utilize boundary polarized (BP) SAW. Here, the dominating mechanical displacement component is within the plane of SAW propagation. Such in-plane components of SAW displacement suffer less attenuation during transmission of the vessel wall since the momentum transfer for both components (longitudinal and shear) is significantly lower (Fig. 1).

However, BP SAW needs to be converted into VP SAW after transmission of the vessel wall in order to achieve desired microfluidic actuation purposes, i.e. to radiate a bulk acoustic wave (BAW) into the fluid yielding to acoustic streaming or giving rise to radiation force on particles/cells inside the fluid, respectively. The polarization conversion can be easily achieved by taking advantage of SAW scattering at the transition from free to metallized substrate surface [2]. The corresponding variation of propagation properties causes the SAW to undergo a change in polarization, i.e. the predominant displacement component switches from in-plane (BP) to out-of-plane (VP). First results of experimental and theoretical investigations of the polarization conversion due to the presence of such a scattering structure are presented and discussed.

II. SETUP AND METHODS

A. SAW devices

The SAW devices used for theoretical and experimental investigations consist of a single crystal lithium niobate substrate (64° rotated Y-cut with X-propagation direction: 64YX $LiNbO_3$, thickness 510 µm) and an aluminum electrode metallization system (layer thickness 300 nm) on top. The SAW excited on 64YX $LiNbO_3$ is characterized by a shear-horizontal polarization. Thus, the in-plane displacement component perpendicular to the SAW propagation direction is the dominating one, whereas the out-of-plane, i.e. the surface-normal component is quite low [2].

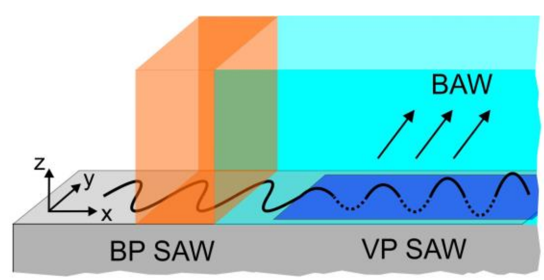

Fig. 1. Principle scheme of SAW polarization conversion used for mircofluidic actuation purposes: a boundary polarized (BP) SAW is excited, passes the vessel wall (orange) and is subsequently converted to a vertical polarized (VP) SAW by undergoing scattering (dark blue) before it radiates a BAW into the fluid (blue). SAW propagation direction is from left to right.

This wave propagates much faster than the quasi-shear bulk wave and thus, is a leaky SAW (LSAW) due to its attenuation caused by the radiation of the bulk wave into the substrate depth. The layout of the metallization system is based on an interdigital transducer (IDT) and an optional metallized area (scattering structure) in front of the IDT with respect to SAW propagation direction. Two different λ/4-IDT designs are realized, one with a period of λ=30 µm and a total number of 14 electrode pairs, and one with a period of λ=120 µm and a total number of 22 electrode pairs. The aperture of both IDTs is 2 mm and the metallization ratio is 0.5. The scattering structure in front of the IDTs starts at a distance of 1 mm (λ=30 µm) and 3 mm (λ=120 µm), respectively. The region between the IDT and the metallized area has free substrate surface. The direct comparison of SAW propagation in presence/absence of the scattering structure allows for the explicit investigation of polarization conversion. SAW devices are fabricated via electron-beam evaporation and lift-off technique of subsequent layers of titanium (5 nm) and aluminum (295 nm).

Besides primary fabrication procedure, the SAW devices need to be additionally prepared. Therefore, the back side of the $LiNbO_3$ substrate is waffled by arranging parallel cuts of 100 µm depth oriented at ±45° w.r.t. to the crystal's X-axis within the region of the IDT. Hence, the propagation of bulk waves that are also excited by the IDT within the substrate material will be suppressed and superposition with the intended surface waves is reduced. Furthermore, the edges of the substrate parallel to the IDT's electrodes are beveled by grinding in order to suppress reflections of the SAW. The back side as well as all surrounding edges of the SAW devices are subsequently covered with highly viscous photo resist to provide additional damping.

B. Experiments

The SAW devices are mounted on a custom designed chip holder to ensure both, mechanical fixation and electrical contact. Electrical characterization is realized in terms of one-port S-parameter measurements by means of a vector network analyzer (VNA, Agilent E5071C, USA). The surface-normal component of mechanical displacement is measured using a Laser Doppler vibrometer (LDV, UHF 120, Polytec, Germany). With this LDV system a pointwise measurement at different positions along the surface is realized in order to achieve the lateral distribution of displacement amplitude. The region under investigation of the SAW devices is chosen to cover the area in front of the IDT w.r.t. SAW propagation direction, i.e. line scans at the center of aperture and parallel to SAW propagation direction with a point-to-point distance Δx=3 µm (λ=30 µm) and Δx= 6 µm (λ=120 µm) are performed.

C. Theoretical model and computations

The acoustoelectric fields are computed by the finite element method (FEM). The model considers that the electrodes are infinitely long in the direction of y-axis which is perpendicular to the direction of wave propagation (x-axis). The number of electrodes, the period of the grating, and the metallization ratio as well as the thickness of electrodes and homogeneous metal film are the same as in the samples used for experiments. The computational domain includes the full IDT and the metal film, if the latter is present and it is surrounded by perfectly matched layers (PML) from the bottom and both left-hand and right-hand sides. If the surface is not metallized, then the symmetry of the substrate – the mirror plane is perpendicular to the direction of propagation – allows to simulate only a half of the structure, e.g. its right-hand side. In this instance the PML is placed only at the bottom and the right-hand edge of the computational domain, while special boundary conditions are set on its left-hand edge, namely, $u_2 = u_3 = \varphi = \sigma_{11} = 0$, where u_i, i = 1, 2, 3, are the components of the mechanical displacement $\mathbf{u}$, φ is the electric potential and σ_{11} is 11-component of the mechanical stress tensor $\boldsymbol{\sigma}$ [3]. The program is written on the basis of Comsol Multiphysics 3.5a. It solves the stationary equations of piezoacoustics in the domains corresponding to the substrate and "substrate" PMLs, the equations of elastodynamics in the electrodes and metal film, and the Laplace equation in the vacuum and "vacuum" PMLs. Given the frequency and the voltage on the electrodes, the mechanical displacement and the electric potential as function of the coordinates x and z are computed, where xz-plane is the sagittal plane.

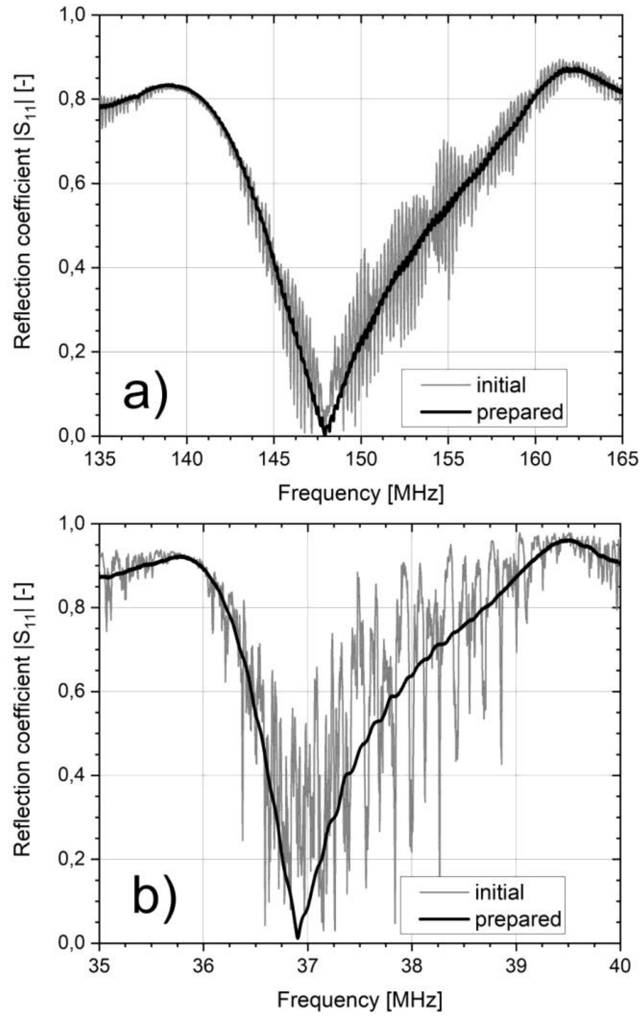

Fig. 2. Electrical characterization of SAW devices in terms of frequency dependent reflection coefficient $|S_{11}|$: a) λ=30 µm and b) λ=120 µm, both with metallized area in front of the IDT. Additional sample preparation yields effective suppression of acoustic reflections from edges and the back side of the substrate (black curves) compared to the initial state (gray curves).

III. RESULTS

A. Electrical characterization

Electrical characterization of SAW devices yields the typical, frequency-selective behavior for IDT on piezoelectric substrate (Fig. 2). The $|S_{11}|$ minimum frequency, indicating a nearly perfectly matched impedance (50 Ω), is approximately 37 MHz (λ=120 µm) and 148 MHz (λ=30 µm), respectively. However, for both cases the synchronous frequency of the IDT is slightly higher. The presence/absence of the metallized area in front of the IDT does not influence the general electrical behavior. Therefore, Fig. 2 shows results for different SAW wavelengths, both in presence of the metallized area. The initial state of the samples is characterized by distortions of the characteristics resulting from surface wave reflections at the substrate edges as well as from bulk wave reflections at the back side of the substrate. To overcome this, an additional sample preparation is performed capable to efficiently suppress these parasitic wave components and allowing for experimentally investigating the SAW modes only.

B. Displacement amplitude

Investigations of the displacement amplitude are performed at $|S_{11}|$ minimum frequencies in order to achieve maximum SAW amplitude. Furthermore, the electrical voltage applied to the IDT during LDV measurements is determined and subsequently used for computations of displacement amplitude (Tab. I). This procedure allows for a direct comparison between out-of-plane displacement amplitudes of experiment and simulation (Fig. 3). In general, the absolute value of displacement amplitude obtained from numerical computations is in good agreement with LDV measurement results. Thus, the model is capable to adequately account for the electroacoustic transmission behavior of the IDT-substrate combination as well as for the presence of a surface metallization in front of the IDT.

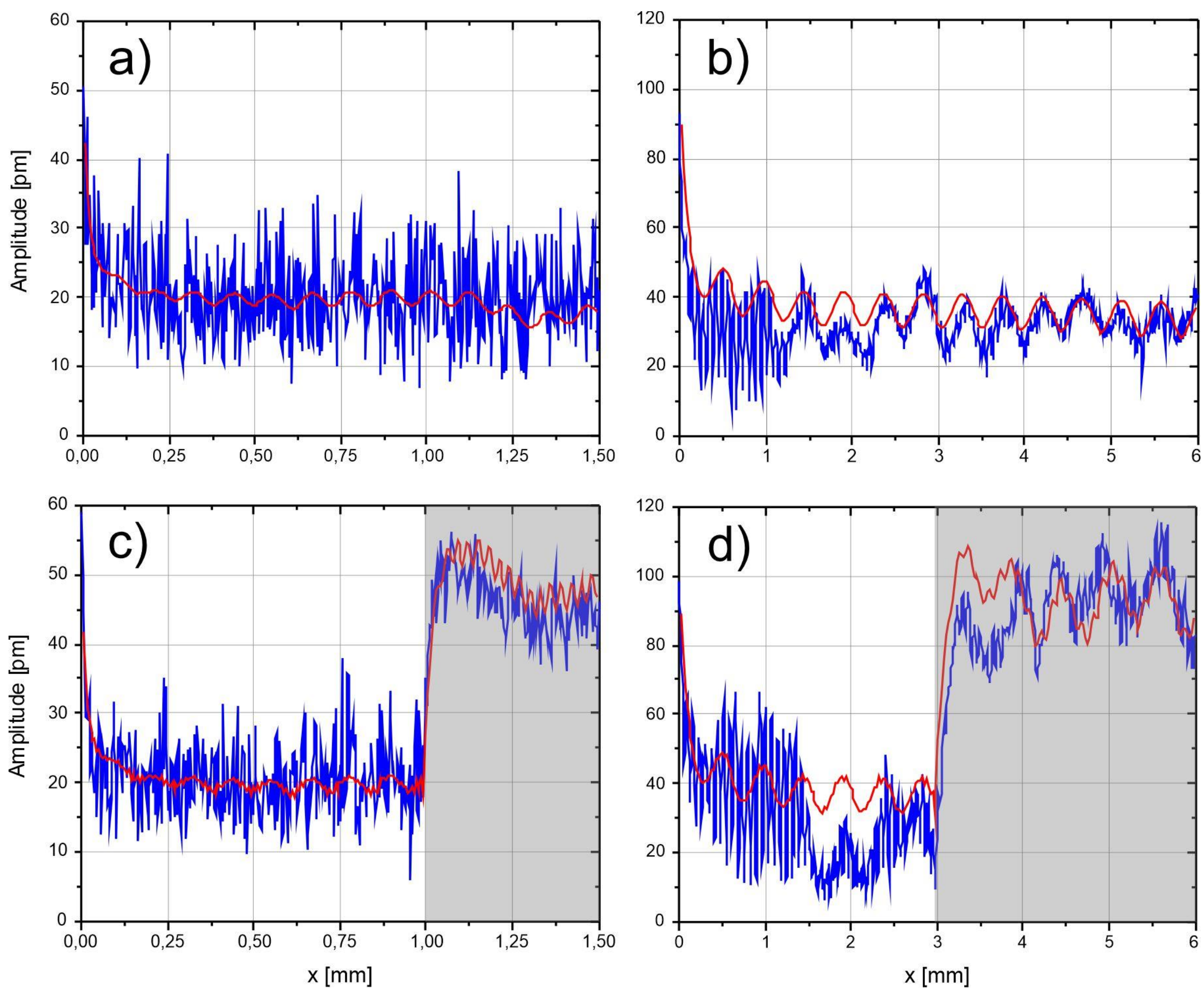

Fig. 3. Out-of-plane SAW displacement amplitude in front of IDTs: a) λ=30 µm **w/o** metal, b) λ=120 µm **w/o** metal, c) λ=30 µm **with** metal and d) λ=120 µm **with** metal (the metallized scattering area is indicated in gray). Line scans are performed at the center of aperture with the last IDT electrode located at x=0. Simulation results (red curves) are computed for the same frequency and voltage (Tab. I) as applied to the SAW device during LDV measurement (blue curves).

TABLE I. PARAMETERS USED FOR EXPERIMENTAL AND NUMERICAL INVESTIGATIONS OF SAW DISPLACEMENT AMPLITUDE

IDT period [µm]	Frequency [MHz]	Voltage [V]	Gap [mm]
30	148	1.25	1
120	37	1.21	3

The presence of this metallized area provokes an abrupt increase of the out-of-plane component of SAW amplitude by a factor 2.5, both for λ=30 µm and λ=120 µm (Fig. 3c, d). The amplitude changes within a couple of wavelengths leading to an almost stepwise increase. Increased amplitude fluctuations are obvious for λ=30 µm, especially at the free substrate surface (Fig. 3a, b), caused by low out-of-plane displacement amplitudes leading to a low signal-to-noise ratio (SNR) during measurement. Nevertheless, the mean value still shows good agreement with the computed curve even though the small periodic variations predicted by computations cannot be seen from measured data. The higher the amplitude the lower is the uncertainty of LDV measurement results. Fluctuations due to low SNR decrease for amplitudes greater than 30 pm. Small-scale periodic variations of amplitude can be identified both, from experimental and theoretical results for λ=120 µm which are in good agreement (Fig. 3b, d). However, relevant discrepancies between measurement and computation can be stated for the area directly in front of the IDT (λ=120 µm, x<3 mm).

IV. CONCLUSION

Surface-normal displacement amplitude can be reliably measured even in case of shear-horizontal polarized SAW with low surface-normal component of mechanical displacement. As expected, the presence of a scattering structure (metallized substrate surface) causes significant change of the polarization of a boundary polarized SAW yielding an increased out-of-plane displacement component. Investigations are limited to the unloaded (bare) surface of SAW devices so far, i.e. without any fluid or polymer. Future work will incorporate the presence of necessary microfluidic components. However, the presented results clearly depict, that the approach of SAW scattering is suitable to achieve relevant polarization conversion. Moreover, it also allows for the spatial control of acoustofluidic interaction since the geometry of the scattering structure is designable on demand, i.e. there is free choice of the lateral dimensions as well as of the positions of scatterers inside a microfluidic vessel. This gives an additional degree of freedom for realizing tailored SAW-driven microscale actuation devices. It should be mentioned that some polarization conversion of BP SAW may also occur at the transition from the vessel wall to the fluid loaded surface due to the change of dielectric permittivity from vessel wall material to fluid. Beside mechanical displacements, the propagation of SAW on piezoelectric substrates is accompanied by an electric field that is affected by the dielectric permittivity of the exterior space, i.e. the material in contact with the substrate surface [2].

ACKNOWLEDGMENT

The authors thank German Research Foundation (DFG grant SCHM2365/16-1) for financial support. The work of A.D. was also supported by the Ministry of Science and Higher Education of the Russian Federation.

REFERENCES

[1] D.B. Go, M.Z. Atashbar, Z. Ramshani, and H.-Ch. Chang, Surface acoustic wave devices for chemical sensing and micro uidics: a review and perspective. Anal. Methods 9, 4112 (2017).

[2] A.N. Darinskii, M. Weihnacht, and H. Schmidt, Acoustomicrofluidic application of quasi-shear surface waves. Ultrasonics 78, 10 (2017).

[3] A.N. Darinskii, M. Weihnacht, and H. Schmidt, Usage of symmetry in the simulation of interdigital transducers, IEEE Trans. Ultrason., Ferroelect., Freq. Contr. 57, 2356 (2010).